



Lipocalin 2 as a Putative Modulator of Local Inflammatory Processes in the Spinal Cord and Component of Organ Cross talk After Spinal Cord Injury

Victoria Behrens¹ · Clara Voelz¹ · Nina Müller¹ · Weiyi Zhao¹ · Natalie Gasterich¹ · Tim Clarner¹ · Cordian Beyer¹ · Adib Zendedel^{1,2}

Received: 17 May 2021 / Accepted: 9 August 2021 / Published online: 21 August 2021
© The Author(s), under exclusive licence to Springer Science+Business Media, LLC, part of Springer Nature 2021

Abstract

Lipocalin 2 (LCN2), an immunomodulator, regulates various cellular processes such as iron transport and defense against bacterial infection. Under pathological conditions, LCN2 promotes neuroinflammation via the recruitment and activation of immune cells and glia, particularly microglia and astrocytes. Although it seems to have a negative influence on the functional outcome in spinal cord injury (SCI), the extent of its involvement in SCI and the underlying mechanisms are not yet fully known. In this study, using a SCI contusion mouse model, we first investigated the expression pattern of Lcn2 in different parts of the CNS (spinal cord and brain) and in the liver and its concentration in blood serum. Interestingly, we could note a significant increase in LCN2 throughout the whole spinal cord, in the brain, liver, and blood serum. This demonstrates the diversity of its possible sites of action in SCI. Furthermore, genetic deficiency of Lcn2 (Lcn2^{-/-}) significantly reduced certain aspects of gliosis in the SCI-mice. Taken together, our studies provide first valuable hints, suggesting that LCN2 is involved in the local and systemic effects post SCI, and might modulate the impairment of different peripheral organs after injury.

Keywords Spinal cord · Astroglia · Lipocalin 2 · Organ cross talk

Abbreviations

ALDH1L1	Aldehyde dehydrogenase 1 family member L1	GAPDH	Glyceraldehyde 3-phosphate dehydrogenase
Bax	Bcl-2-associated X protein	Hsp90	Heat shock protein 90
Bcl2	B-Cell lymphoma 2	IBA1	Ionized calcium binding adaptor molecule 1
BSA	Bovine serum albumin	IgG	Immunoglobulin G
C3	Complement component 3	LCN2	Lipocalin 2
CD31	Cluster of differentiation 31	M-MLV	Moloney murine leukemia virus
CD44	Cluster of differentiation 44	NGAL	Neutrophil gelatinase-associated lipocalin
CNS	Central nervous system	PBS	Phosphate-buffered saline
EDTA	Ethylenediaminetetraacetic acid	PCR	Polymerase chain reaction
ELISA	Enzyme-linked immunosorbent assay	PFA	Paraformaldehyde
FCS	Fetal calf serum	PVDF	Polyvinylidene difluoride
GFAP	Glial fibrillary acidic protein	RIPA	Radioimmunoprecipitation assay
		RT	Room temperature
		SC	Spinal cord
		SCI	Spinal cord injury
		SDS	Sodium dodecyl sulfate
		SPHK1	Sphingosine kinase 1
		TBS	Tris-buffered saline
		WT	Wild-type

✉ Adib Zendedel
azendedel@ukaachen.de

¹ Institute of Neuroanatomy, RWTH Aachen University, 52074 Aachen, Germany

² Department of Anatomy, School of Medicine, Tehran University of Medical Sciences, Tehran, Iran

Introduction

Spinal cord injury (SCI) is a devastating event that causes life-long health restrictions including paralysis, loss of sensation and vegetative functions, pain, and psychological impairment [1]. Despite many efforts, there is presently no comprehensive treatment protocol available to effectively treat this injury, mainly owed to the complexity of nerve fiber tract destructions, neuronal death, and poor restoration capacities of physiological function [2, 3]. In SCI, the primary injury refers to the initial physical damage of the spinal cord (SC), which is accompanied by hemorrhage, ischemia, and local neuronal death, while the secondary injury phase is characterized by progressive damage of the SC, demyelination, astrogliosis, and neuroinflammation [4–9]. Progressing neuroinflammation, which is a major hallmark of the secondary injury, is mainly initiated through activation of astrocytes and microglia, which are key cells in the maintenance of homeostasis in the CNS, and further boosted and perpetuated by infiltrated neutrophils and macrophages [10–13]. The activation of astrocytes and microglia, so-called astrogliosis and microgliosis, respectively, influences the disease outcome in SCI on various levels [14, 15].

Astrocytes are the predominant subtype of glial cells in the CNS. Under physiological conditions, they protect neurons through the uptake of excessive neurotransmitters, i.e., glutamate, maintain the integrity of the blood–brain barrier and participate in synaptic stability, plasticity, and reorganization [16, 17]. When being activated, astrocytes become hypertrophic and develop extended processes [6]. Reactive astrocytes are a central component of the glial scar which is formed around the injury site in the secondary injury phase [18]. Glial scar formation affects the healing process and can remain chronically for up to several decades in patients who suffered from SCI [14]. The glial scar limits the spread of inflammation but, at the same time, impedes axonal regeneration [19–21]. Under pathological conditions such as traumatic SCI, reactive astrocytes promote cytotoxic edema formation and ischemia through an upregulation of aquaporin 4 [16]. Furthermore, they are an integral component of local immune responses by producing and secreting a wide range of cytokines and chemokines [22, 23]. It has been shown that the phenotype of reactive astrocytes varies, and it has been assumed that astrocytes can differentiate in the direction of either a more pro-inflammatory A1 or a more anti-inflammatory A2 polarization state [24]. A1 polarized astrocytes express pro-inflammatory cytokines and contribute to neuronal death, whereas A2 polarized astrocytes stimulate CNS recovery and repair [24, 25].

The neuroinflammation in SCI is regulated by expression of pro-inflammatory and anti-inflammatory cytokines, chemokines, and other mediators, which are mainly

synthesized by glial cells. The glycoprotein lipocalin 2 (LCN2) is considered a key mediator of immune responses in general and particularly in neurodegenerative diseases [26–31]. It has been shown that LCN2, which is upregulated at the lesion site of the SC, is produced by astrocytes after SCI [26]. Furthermore, *Lcn2*-deficient mice reveal better functional outcomes, a lower expression of chemokines, and a reduced extent of secondary injury after SCI in comparison to wild-type mice [26]. In general terms, LCN2 plays an important role in iron transport and homeostasis and promotes the defense against bacterial infections [27, 32]. Furthermore, it has been demonstrated in vitro that LCN2 has toxic effects on neurons and regulates the expression of pro-inflammatory cytokines and chemokines [30, 33]. It has further been stated that LCN2 promotes the shifting of the polarization of microglia and astrocytes towards pro-inflammatory phenotypes in vitro [25, 34].

It has been shown that SCI causes pathological processes in various parts of the body, which were not directly affected by the injury. In patients suffering from SCI cognitive dysfunction, inflammation-associated neurodegeneration of brain tissue and an impaired functional brain recovery are commonly observed [35–37]. In addition to the interaction between different parts of the CNS, a further important issue related to neural injury is the communication with peripheral organ systems, i.e., “CNS-organ cross talk”. There are preliminary findings which show that in SCI, a defined communication axis exists between SC and liver suggesting that the liver might exhibit mechanisms that influence neuroinflammation in the SC [38, 39].

Due to the limited treatment options in SCI, it is important to identify new possible drug targets. As we suggest LCN2 to influence SCI pathology, it is of interest to examine its effects on astrocytes, which play a central role in SCI pathology. Additionally, we wanted to get a first impression of whether LCN2 might participate in the systemic effects of SCI. In the present study, we have analyzed the time course of local *Lcn2* expression post SCI and its influence on the activation and polarization of astrocytes. Furthermore, since LCN2 is also secreted in a paracrine and endocrine fashion, we analyzed the amount of LCN2 in blood and other peripheral organs post SCI.

Materials and Methods

Animals

We used male C57BL/6JRj wild-type mice (WT) and mice carrying a general *Lcn2* deficiency (*Lcn2*^{-/-}) at the age of 8–14 weeks.

The mice were housed and handled in accordance with the guidelines of the Federation for European Laboratory Animal Science Associations (FELASA) under standard laboratory conditions. The procedures were approved by the Review Board for the Care of Animal Subjects of the district government (North Rhine-Westphalia, Germany) and performed according to international guidelines on the use of laboratory mice (Az 81–02.04.2018.A227). *Lcn2*^{-/-} mice of the 7-day group were approved by the Review Board for the Care of Animal Subjects of the district government (ethic No. 962055, Tehran, Iran).

The WT mice were obtained from Janvier Labs (Saint-Berthevin Cedex, France); information on the genetic identification of the WT mice is available on their homepage (<https://www.janvier-labs.com/en/an-optimal-management-of-genetics-a-unique-concept/>). The Janvier Labs' colony belongs to a genetically tested and characterized founding pair (genetic analysis 640,000 SNPs) that is identical to that of the C57BL/6JRj. *Lcn2*-deficient mice (*Lcn2*^{-/-}), which have already been used in other studies from our group, were kindly provided by Tak W Mak (University of Toronto, Canada) and colleagues [30, 40, 41]. In these mice, a targeted mutation has been introduced to disrupt the *Lcn2* coding region, including exons 1–5, with a PGK-neo cassette, thus leading to a functional knockout in all tissues including the CNS. For breeding, pairs of homozygous mice were used.

Spinal Cord Injury

General anesthesia was initiated with isoflurane (2–3 vol%) in an anesthetic chamber. During surgery, isoflurane (1.5–2 vol%) was further administered via a face mask. Intraoperative analgesia was attained through injection of buprenorphine (0.05–1 mg/kg s.c.) 30 min preoperatively. After the exposure of the spinal column (T7–T10), a laminectomy of T8 was performed. A standardized injury of the SC at this level was induced by contusion (Infinite Horizons Spinal Cord Impactor) with a force of 60 kdyn. After inducing the SCI, the surgical site was sutured in layers and the mice were injected subcutaneously with sterile saline. Postoperative care involved the daily manual emptying of the bladder until spontaneous urination returned. In the control group, after preoperative analgesia and general anesthesia as described above, the spinal column (T7–T10) was exposed, and a laminectomy of T8 was performed. The surgical site was then sutured in layers, and the mice were injected subcutaneously with sterile saline. Through this approach, we aim to preclude possible falsifications of the results caused by the mere surgical procedure.

BBB Scoring

To assess functional recovery and locomotion deficits after SCI, the mice were scored in an open field according to

Basso, Beattie, and Bresnahan (BBB) locomotion rating scale of 0 (complete paralysis) to 21 (normal) as previously described [42]. The scale assesses hind limb movements, body weight support, forelimb to hind limb coordination, and whole-body movements.

Tissue Preparation

At defined time points after SCI (6, 12, 24, 72, h and 7 days), the mice were transcardially perfused with ice-cold PBS for molecular biological and protein biochemical studies. The sham-operated mice, which served as control, were finalized after 24 h. The whole SC was prepared and divided into three parts, in the following referred to as rostral, central (lesion site), and caudal region. The three spinal cord regions were separated at the level of T3 and L1. This ensures that the caudal and rostral regions are located at a sufficient distance of several millimeters from the visually visible lesion area.

In addition, motor and sensory cortex and left liver lobe were prepared. The tissues were immediately snap frozen in liquid nitrogen and kept at –80 °C until further processing.

For immunohistochemistry, the mice (control, 24 h, 72 h, and 7 days) were transcardially perfused with ice-cold PBS followed by a 3.7% paraformaldehyde solution (PFA, pH 7.4). For decalcification, spinal columns were incubated in 20% EDTA (ethylenediaminetetraacetic acid) for 48 h at 37 °C prior to paraffin embedding. Tissue specimens were cut into three parts, as described above, and embedded in paraffin (Merck, Darmstadt, Germany). Five-micrometer paraffin sections were cut. Blood sampling (control, 6, 12, 24, 72 h, and 7 days) was performed through retro-bulbar sinus puncture.

Molecular Biological Analysis

For RNA isolation, the tissues were placed in homogenization tubes containing 1.4-mm beads. Samples were homogenized at 5000 × g for 15 s. RNA was isolated by phenol–chloroform extraction using peqGold RNA Tri-Fast (PeqLab, Erlangen, Germany). Total RNA amount and purity are determined using 260/280 ratios of optical densities (Nanodrop 1000, PeqLab, Erlangen, Germany). cDNA was obtained by reverse transcription using M-MLV reverse transcription (RT) kit and random hexanucleotide primers (Invitrogen, Carlsbad, USA). Gene expression levels were analyzed with real-time reverse transcription-PCR (Bio-Rad, Feldkirchen, Germany) using SensiMix™ SYBR® & Fluorescein Kit (Meridian Bioscience, Cincinnati, USA). Distilled water was used instead of cDNA as negative control. Primer sequences and individual annealing temperatures are shown in Table 1. Results were evaluated using Bio-Rad CFX manager (Bio-Rad, Feldkirchen, Germany) and were normalized to cyclophilin A and Hsp90 as reference genes.

Table 1 List of primers used in this study

Primer	Sense	Anti-sense	Annealing temperature (°C)
Bax	GGCAGACAGTGACCATCTTT	AGTGGACCAGAGGTTTATTG	59
Bcl2	CGATCAATCAAAGCCAAGCA	AGCCTTCAGGCAAGTTCAGG	62
C3	TCCAATGTCCTACGGCTG	ACGTAATGTGCCCCCTCCTT	60
Cyclophilin A	TTGGGTCCAGGAATGGCAAGA	ACATTGCGAGCAGATGGGGT	64
Gfap	GAGATGATGGAGCTCAATGACC	CTGGATCTCCTCCTCCAGCGA	60
Hsp90	TACTACTACTCGGCTTCCCGT	TCGAATCTTGTCCAGGGCATC	64
Lcn2	GCAGGTGGTACGTTGTGGG	CTCTTGTAGCTCATAGATGGTGC	65
Serpina3n	AACCAGAGACCCTGAGGAAGT	AGTTTCGAGACATTGGGACAA	60
Sphk1	TATGCTGGGTACGAGCAGGT	CCCCTGTGAAACGAATCTCC	65
Vimentin	ATGCTTCTCTGGCACGTCTT	AGCCACGCTTTCATACTGCT	65

The target gene expression was calculated using the $\Delta\Delta C_t$ method [43].

Protein Biochemical Analysis

Sampled tissues were mechanically disrupted in RIPA buffer (pH 8.0) supplemented with a protease inhibitor cocktail (Complete Mini, Roche Diagnostics, Grenzach-Wyhlen, Germany). Protein concentrations were determined using the Pierce™ BCA Protein Assay kit (Thermo Fisher Scientific, Waltham, USA) according to the manufacturer's protocol. Per sample, a total of 20 µg protein was separated in a 14% SDS polyacrylamide gel by gel electrophoresis and transferred to a PVDF (polyvinylidene difluoride) membrane. The blots were blocked in 5% milk in tris-buffered saline (TBS, pH 7.4) and then incubated overnight (at 4 °C) in primary antibodies rabbit anti-LCN2 in 5% milk and rabbit anti-GAPDH in 5%

milk (used antibodies are listed in Table 2). An appropriate secondary antibody (goat anti-rabbit IgG (H + L)-HRP) was applied for 2 h (RT). Signals were analyzed via chemiluminescence detection (Westar Supernova, XLS 3,0100, Cyanagen, Bologna, Italy), visualized (Fusion Solo X, Vilber, Eberhardzell, Germany) and subjected to densitometry analysis using Image J. Results were normalized to GAPDH as reference protein.

ELISA

Concentrations of LCN2 in serum were assessed using mouse LCN2/NGAL Quantikine ELISA Kit (R&D Systems, Minneapolis, USA) according to the manufacturer's protocol. Samples were assayed in duplicates and used in a 200-fold (control), respectively 500-fold (6, 12, 24, 72 h, and 7 days) dilution. Absorbance was measured using a

Table 2 List of antibodies used in this study. WB Western Blot; IHC Immunohistochemistry; IF Immunofluorescence

	Antibody	Host species	Manufacturer	WB	IHC	IF
Primary antibodies	LCN2	Rabbit	Cloud-Clone Corp., Houston, USA	1:500	1:500	1:500
	GAPDH	Rabbit	Santa Cruz, Dallas, USA	1:5000		
	IBA1	Mouse	Merck Millipore, Burlington, USA			1:600
	CD44	Rat	BD Biosciences, Franklin Lakes, USA			1:50
	GFAP	Goat	Santa Cruz, Dallas, USA			1:100
	CD31	Rat	Dianova, Hamburg, Germany			1:100
	ALDH1L1	Rabbit	Abcam, Cambridge, UK		1:1000	
Secondary antibodies	Anti-rabbit IgG (H + L)-HRP	Goat	BIO-RAD, Feldkirchen, Germany	1:50,000		
	Anti-rabbit IgG (H&L)	Goat	Vector Labs, Burlingame, USA		1:50	
	Anti-rabbit 488	Donkey	Life Technologies, Carlsbad, USA			1:500
	Anti-goat 594	Donkey	Life Technologies, Carlsbad, USA			1:500
	Anti-mouse 594	Donkey	Life Technologies, Carlsbad, USA			1:500
	Anti-rat 555	Goat	Invitrogen, Carlsbad, USA			1:500

microplate reader (Tecan GmbH, Männedorf, Switzerland). Final concentrations were calculated from a standard curve.

Immunohistochemistry

For immunohistochemistry (IHC), 5- μ m thick sections of SC, brain, and liver were rehydrated, and antigens were unmasked by heating in Tris/EDTA (pH 9.0) buffer for 20 min. After blocking with 5% normal goat serum in PBS, the sections were incubated overnight (4 °C) with rabbit anti-LCN2, or rabbit anti-ALDH1L1 respectively, diluted in 5% normal serum in PBS. Slides were incubated for 30 min in 0.3% H₂O₂ (in PBS) followed by incubation with goat anti-rabbit IgG (H&L) diluted in 5% normal serum in PBS for 1 h (RT). Afterwards, an incubation with ABC-solution (both parts 1:50, VECTASTAIN Elite ABC Kit (Standard), Vector Labs, Burlingame, USA) diluted in PBS for 1 h (RT) followed.

For double immunofluorescence labeling, sections were blocked with IFF buffer, containing BSA, FCS and 1 \times PBS, for 1 h and incubated overnight (4 °C) with rabbit anti-LCN2 diluted in IFF buffer. The slides were incubated with donkey anti-rabbit 488 diluted in IFF buffer for 1 h (RT) followed by an incubation with goat anti-GFAP, respectively mouse anti-IBA1, rat anti-CD44, or rat anti-CD31 diluted in IFF buffer overnight (4 °C). Finally, the slides were incubated with donkey anti-goat 594, respectively donkey anti-mouse 594 or goat anti-rat 555 in IFF buffer for 1 h (RT). As negative controls, slices of the examined tissue, which were not incubated with the respective primary antibodies, were used. Apart from that, the negative controls were treated like the stained slices.

Statistical Analysis

A total of 59 WT animals were used for the experiments containing 43 animals for qPCR analysis. Twenty-four out of the 43 animals were also used for western blot analysis. Samples from 39 animals were subjected to ELISA. For immunohistochemistry staining, we used slices from 16 animals. A total of 20 Lcn2^{-/-} mice were used for qPCR analysis and 4 for immunohistochemistry. Per group, 4 animals and 3 sections per animal at a distance of 100 μ m were stained.

GraphPad Prism 8 (GraphPad Software Inc., San Diego, USA) was used for statistical analysis. Brown-Forsythe test was performed to test for equal variances and normal distribution was tested with Shapiro–Wilk’s test. If necessary, data were transformed via Boxcox for homoscedasticity. One-way ANOVA followed by Dunnett’s post hoc test or two-way ANOVA followed by Tukey’s post hoc test was used for parametric data. Non-parametric data (Lcn2

mRNA in sensory and motor cortex and LCN2 concentration in blood serum) were analyzed with the Kruskal–Wallis test followed by Dunn’s multiple comparisons. WT and Lcn2^{-/-} data from BBB scoring were compared by two-way ANOVA with Geisser–Greenhouse correction. All data are given as arithmetic means \pm standard errors of the mean (SEM). The *p* values were set as **p* \leq 0.05, ***p* \leq 0.01, ****p* \leq 0.001, and *****p* \leq 0.0001, respectively #*p* \leq 0.05, ##*p* \leq 0.01, ###*p* \leq 0.001, and ####*p* \leq 0.0001.

Results

In a first set of experiments, we aimed at investigating whether traumatic SCI leads to an increase in Lcn2 expression within the SC and other peripheral organs. Figure 1 shows a significant and stepwise increase of LCN2 in the central region (injury site) of the SC. mRNA expression immediately rose within the first 6 h post injury reaching maximum level at 24 h post SCI and then rapidly declined at 7 days (Fig. 1a). LCN2 protein levels, which were examined by western blot, revealed a similar time course and profile with a short delay compared to mRNA expression, peaking at 72 h post SCI (Fig. 1b/c). To investigate the distribution and localization of LCN2 positive cells in injured SC, immunostaining against LCN2 was performed. Immunohistochemistry showed high numbers of LCN2-positive cells, especially in the gray matter, in the central lesion region 24 h post injury compared to that of the control group (Fig. 1d/e/f). Double immunofluorescence staining revealed that LCN2 signals are associated with GFAP-positive astrocytes occasionally (Fig. 1j/k). IBA1-positive microglia (Fig. 1g) did not co-localize with LCN2 staining in the SC. By staining against the leukocyte marker CD44 and LCN2, co-expression of CD44 could be seen in most LCN2-positive cells 24 h post SCI (Fig. 1h/i).

To determine whether Lcn2 is upregulated in rostral and caudal parts of the spinal cord, we measured the Lcn2 mRNA levels in these regions. The results indicate a massive upregulation of Lcn2 during the initial 6 h in the rostral part which persists until 72 h (Fig. 2a). In the caudal area, we observed a steady upregulation of Lcn2 during the first 7 days post SCI (Fig. 2b).

In a next step, we have examined whether Lcn2 is upregulated in the brain post SCI. In both examined brain regions, sensory and motor cortex, significantly elevated Lcn2 mRNA levels were already present 6 h post SCI and thereafter declined (Fig. 2c/d). Protein levels were analyzed in the sensory cortex (Fig. 2e/f) showing a similar expression pattern as Lcn2 mRNA. As shown in Fig. 2, our results from immunofluorescence staining against LCN2 revealed no reactivity in the brain slices of sham-operated mice, but LCN2 + cells occurred, mainly around vessels,

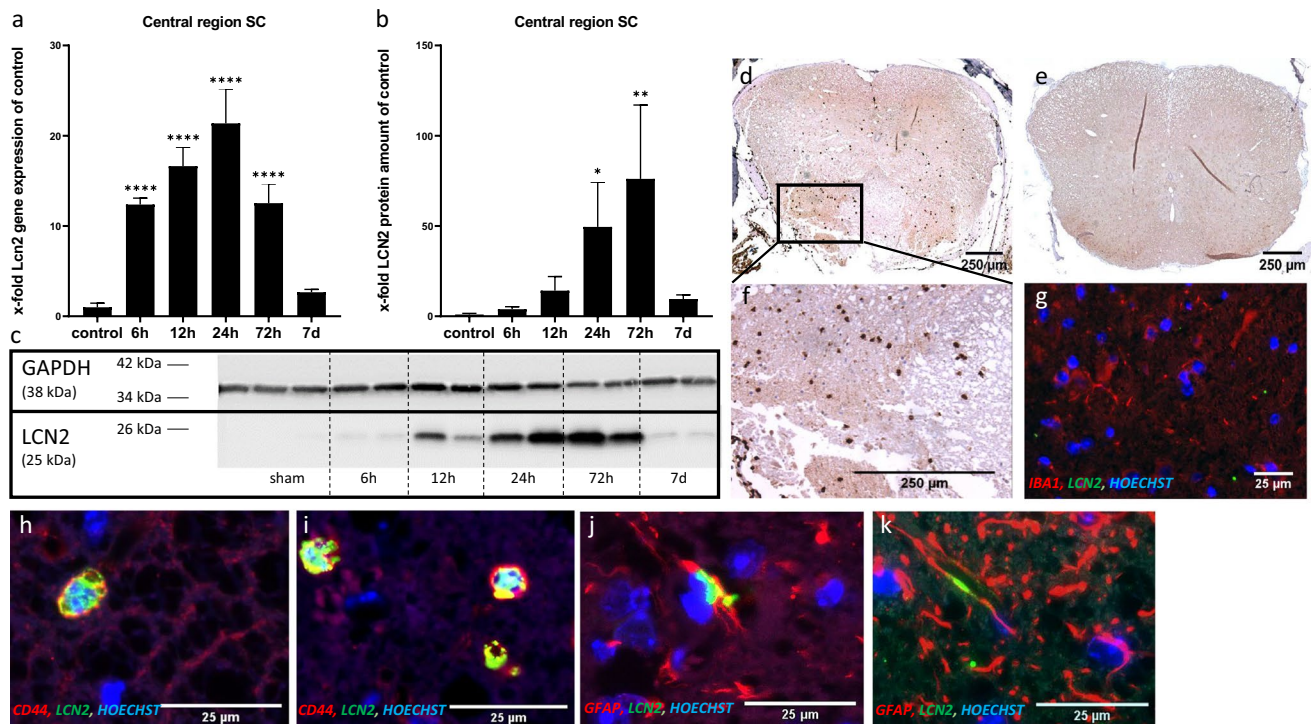


Fig. 1 LCN2 in central region of SC post SCI in WT mice. Lcn2 gene (a) ($n=6$; 72 h, 7 days $n=5$) and protein amount (b/c) ($n=4$). IHC staining against LCN2 of representative sections of the groups 24 h (d/f) and control (e). Double immunofluorescence labeling 24 h

post SCI for LCN2 and IBA1 (g), respectively LCN2 and CD44 (h/i). Double immunofluorescence labeling 24 h post SCI for LCN2 and GFAP (j/k). Data represent means \pm SEM. **** $p < 0.0001$, ** $p < 0.01$, * $p < 0.05$ indicate control vs. time point

after SCI (Fig. 2g/h). To identify these cells as endothelial cells, we performed immunofluorescence double staining, which showed a clear co-localization of LCN2 with the endothelial marker CD31 (Fig. 2i).

Furthermore, we analyzed the LCN2 concentration in blood serum via ELISA, which was significantly elevated around 12 and 24 h post SCI, reaching a ~ 19 -fold increase at its peak (Fig. 3a). In addition, we assessed a potential Lcn2 upregulation in the liver. Here, Lcn2 mRNA (Fig. 3b) and protein (Fig. 3c/d) were significantly elevated from 6 h post SCI on, reaching a peak at 12 h and decreasing again from then on. After immunofluorescence staining, almost no LCN2-immunoreactive cells could be seen in the control group, whereas scattered immunoreaction was detectable after SCI (Fig. 3e/f).

A common phenomenon after SCI is astrogliosis. Since astrocytes are one of the LCN2-producing cell types, we aimed to correlate the expression of astroglial markers (Gfap, vimentin, serpin3n) and Lcn2 in the central SC region (Supplementary Fig. 1a–c). Like Lcn2 mRNA, Gfap, vimentin, and serpin3n mRNA show a significant and progressive increase from 6 h post SCI on. Serpin3n, like Lcn2, reaches its peak at 24 h and decreases from then on, whereas Gfap and vimentin levels proceed to rise.

In order to understand the influence of LCN2 on the pathological scenario after SCI better, we have included animals with a general Lcn2 deficiency (Lcn2^{-/-}) in our study. To assess locomotor impairment and recovery of WT and Lcn2^{-/-} mice after SCI, we used BBB scoring (Fig. 4a). Control animals of both genotypes were all rated with a score of 21, demonstrating their unimpaired condition. At 24 and 72 h, no significant differences in BBB scoring could be seen between the two genotypes. After 7 days, Lcn2^{-/-} mice reached a mean score of ~ 8 , indicating sweeping with no weight support or plantar placement of the paw with no weight support, whereas the mean score of ~ 4 in WT mice stands for only slight movement of all three joints of the hind limbs. The significantly higher scores of Lcn2^{-/-} mice at 7 days indicate better locomotor recovery compared to that of WT mice.

By comparing results from WT and Lcn2^{-/-} tissues, we could first demonstrate that the gene expression of the astrogliosis marker Gfap was reduced in the central SC region of Lcn2^{-/-} animals compared to that of WT mice at all examined time points, with a significant difference between the two genotypes at 24 h (Fig. 4b). Results from staining against the astrocyte marker ALDH1L1 (Supplementary Fig. 2) show fewer positive cells in the lesion region of Lcn2^{-/-} compared to WT at 7 days.

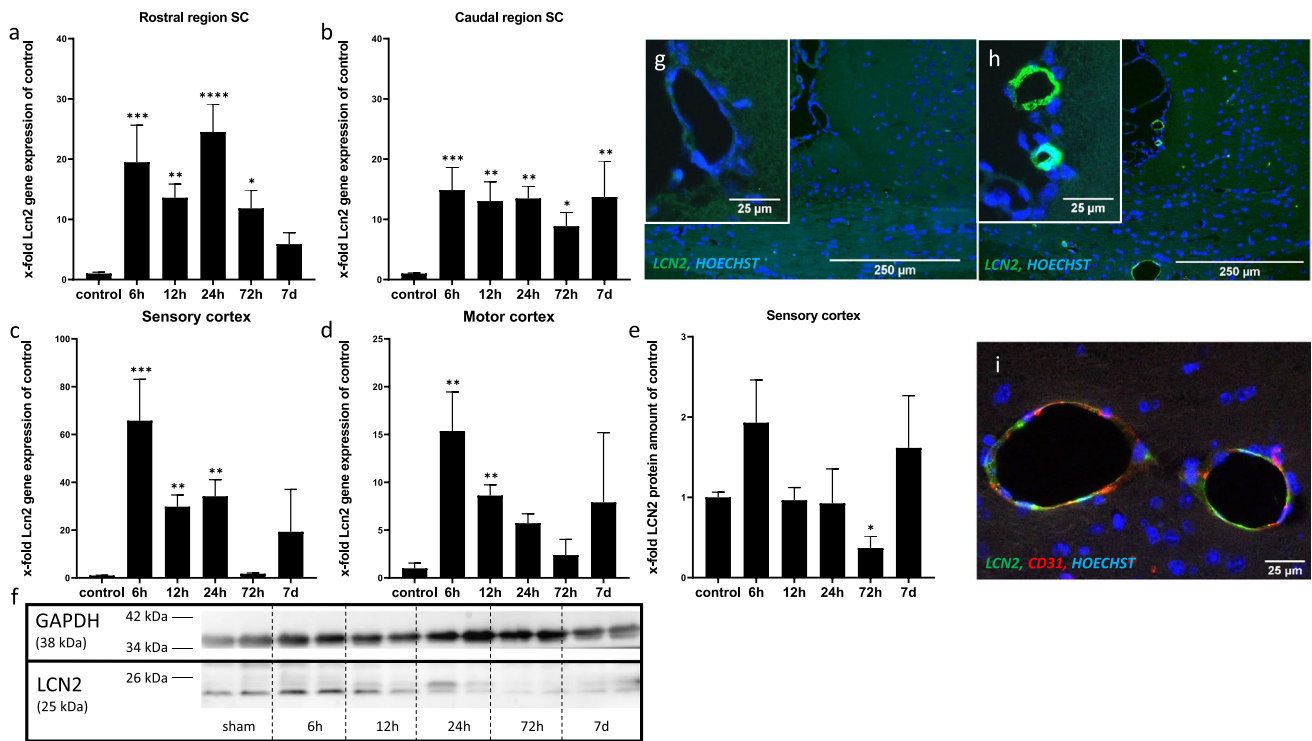


Fig. 2 Lcn2 gene expression in rostral (a) ($n=6$; control $n=5$) and caudal (b) ($n=6$; 7 days $n=5$) region of SC. Lcn2 gene expression in sensory (c) (control $n=5$; 6 h, 12 h, 24 h, 7 days $n=7$; 72 h $n=8$) and motor cortex (d) (control $n=6$; 6 h $n=5$; 12 h $n=8$; 24 h, 72 h, 7 days $n=7$). LCN2 protein amount in sensory cortex (e/f) ($n=4$). Representative brain sections (Bregma—0.82 mm) [86] from control

(g) and 24 h group (h) after IHC staining against LCN2. Representative brain section after double immunofluorescence labeling 24 h post SCI for LCN2 and endothelial marker CD31 (i). Data represent means \pm SEM. **** $p < 0.0001$, *** $p < 0.001$, ** $p < 0.01$, * $p < 0.05$ indicate control vs time point

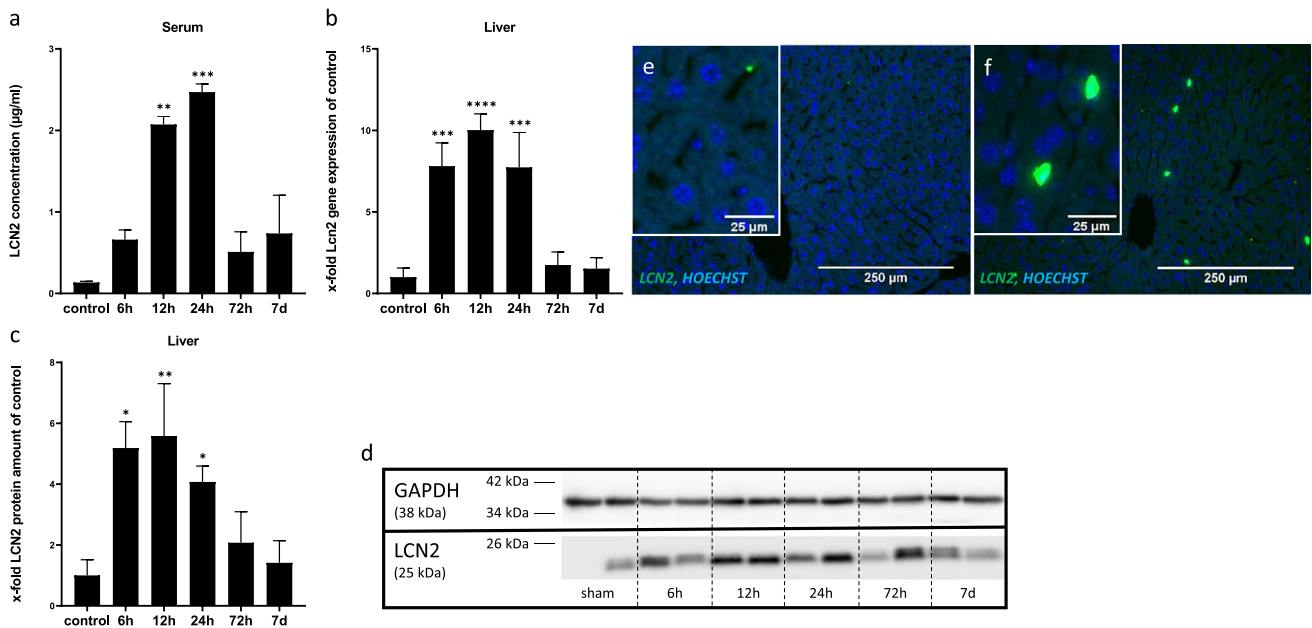


Fig. 3 LCN2 concentration in blood serum (a) (control $n=5$; 6 h $n=6$; 12 h, 24 h, 72 h, 7 days $n=7$). Lcn2 gene expression in liver (b) ($n=5$). LCN2 protein amount in liver (c/d) ($n=4$). Representative liver sections from control (e) and 72 h group (f) immu-

nofluorescence labeled for LCN2. Data represent means \pm SEM. **** $p < 0.0001$, *** $p < 0.001$, ** $p < 0.01$, * $p < 0.05$ indicate control vs time point

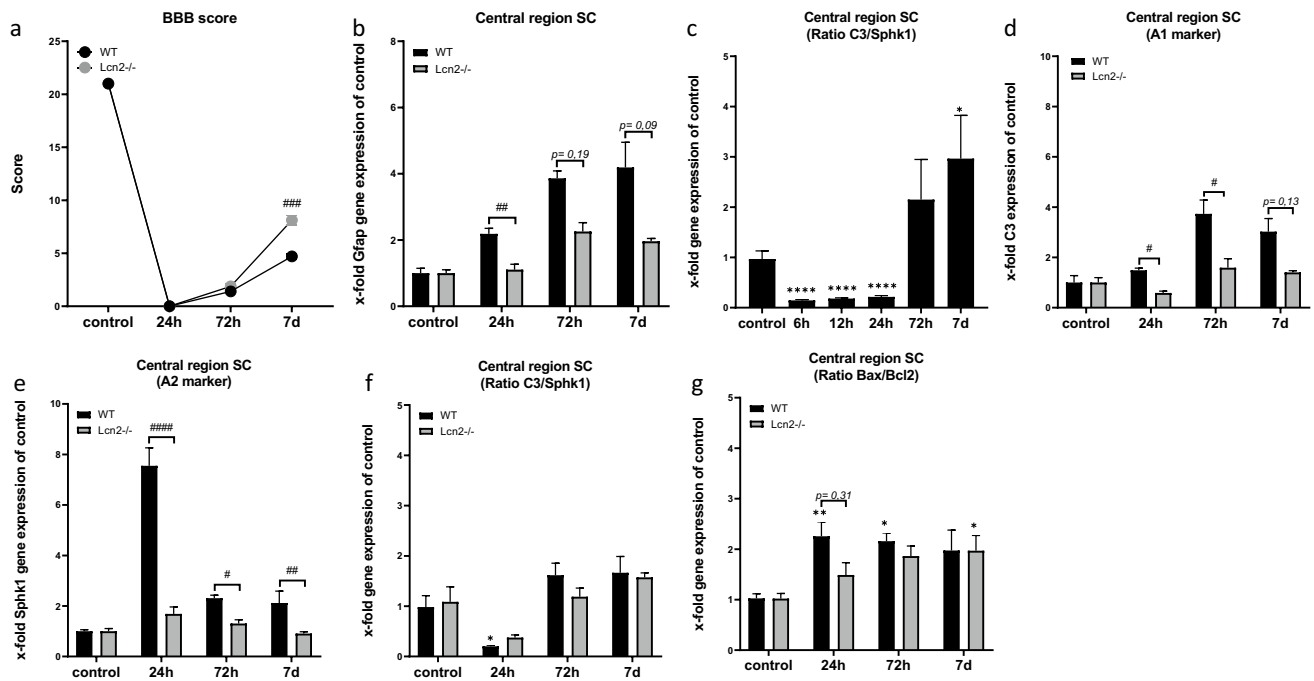


Fig. 4 Comparison of BBB scoring of WT and Lcn2^{-/-} mice post SCI (a) (WT $n=10$; Lcn2^{-/-} $n=8$). Gfap gene expression in WT and Lcn2^{-/-} mice in central (b) ($n=5$) region of SC. Ratio of gene expression of A1 astrocyte marker C3 and A2 astrocyte marker Sphk1 in WT mice (c) ($n=6$). Gene expression of C3 (d) ($n=5$) and Sphk1 (e) ($n=5$) in WT and Lcn2^{-/-} mice in the central region of SC. Ratio of gene expression of C3 and Sphk1 in WT and Lcn2^{-/-} mice (f)

($n=5$). Ratio of gene expression of pro-apoptotic marker Bax and anti-apoptotic marker Bcl2 in WT and Lcn2^{-/-} mice in central region of SC (g) ($n=5$). Data represent means \pm SEM. **** $p < 0.0001$, *** $p < 0.001$, ** $p < 0.01$, * $p < 0.05$ indicate control vs time point (c/f/g), #### $p < 0.0001$, ## $p < 0.01$, # $p < 0.05$ indicate WT vs. Lcn2^{-/-} (a/b/d/e). Wherever a tendency towards a significant difference between WT and Lcn2^{-/-} might be assumed, p values are given

Activated astrocytes can differentiate in the direction of a more pro- or a more anti-inflammatory state and consequently have varying effects on disease pathology. The functional polarization of astrocytes is well-acknowledged. Since LCN2 was shown to influence this polarization in vitro, we also addressed the influence of LCN2 on astrocyte polarization in SCI. Complement component 3 (C3) and sphingosine kinase 1 (Sphk1) were selected as representative markers for A1, respectively A2 astrocyte polarization states. Both markers are well-known and recognized and have been described in publications of renowned journals [24, 44]. Therefore, we analyzed the gene expression profiles of these markers in the injured SC (Fig. 4c–f). In Fig. 4c, a value < 1 of the C3/Sphk1 (A1/A2) quotient indicates a prevalence of A2 during the first 24 h after SCI in the central region in WT mice. From 72 h on, values > 1 demonstrate a prevalence of A1. The underlying individual evaluation of C3 and Sphk1 in WT is not shown. These findings suggest that there are changes in the polarization of astrocytes after SCI.

In order to explore whether LCN2 influences, additionally to the extent of astrogliosis, also the functional polarization of astrocytes, we assessed the mRNA expression of the A1 and A2 markers stated above in Lcn2^{-/-} mice. In the central region of the SC, a significant decrease in A1 and A2 marker

mRNA could be seen at 24 h and 72 h (A1), respectively at all examined time points (A2) in Lcn2^{-/-} mice (Fig. 4d/e). The A1/A2 (C3/Sphk1) quotient in Lcn2^{-/-} shows the same pattern as in WT mice with an initial decrease at 24 h followed by a subsequent increase (Fig. 4f).

To assess the effects of LCN2 on apoptosis rates, the ratio of Bax mRNA, an apoptotic marker, and Bcl2 mRNA, an anti-apoptotic marker, was evaluated in WT and Lcn2^{-/-} mice. As we expected, we observed a significant increase of the Bax/Bcl2 quotient, indicating a pro-apoptotic state, in the central part of the SC at 24 and 72 h in WT mice (Fig. 4g). In contrast, the Bax/Bcl2 quotient did not change significantly compared to the control in the rostral and caudal region (Supplementary Fig. 1d/e). In Lcn2^{-/-} mice, we observed only a slight reduction of Bax/Bcl2 ratios in the central SC region in comparison to WT mice, which did not reach a significant level (Fig. 4g).

Discussion

In the present study, we used a well-established SCI contusion mouse model to provide evidence that LCN2 is upregulated after SCI throughout the whole SC and not only in the

primarily injured region. Beyond SC, we observed a LCN2-induction in the cerebral cortex at both protein and mRNA levels. Interestingly, we show a marked increase of LCN2 in systemic circulation and also in liver in the early phase post SCI. Various studies have found a correlation between increased LCN2 levels and CNS disorders, such as multiple sclerosis and stroke [28, 30, 45, 46]. Therefore, using *Lcn2*^{-/-} mice, we investigate the effect of *Lcn2* deficiency on astrogliosis as a hallmark of SCI. Since the results show a significant reduction of Gfap, a decrease of astrogliosis in *Lcn2*-deficient mice might be concluded.

Post SCI, astrocytes proliferate and undergo morphological changes which include hypertrophy and the development of extended processes [6, 47]. Through the release of neurotrophic factors, astrocytes support neurons in SC and thus, impaired astrocytic function has major consequences for neuronal function [17, 48]. In brain injury, the ablation of reactive astrocytes was found to lead to substantial neuronal degeneration [17]. Moreover, astrocytes limit the spread of inflammation after SCI, since they are one of the dominant cell types of the glial scar which forms after injury [21, 47]. Furthermore, activated astrocytes can express a variety of cytokines, chemokines, and the respective receptors, and therefore play a pivotal role in the neuroinflammatory processes in SCI [47, 49]. Furthermore, axonal regeneration is inhibited by the glial scar and chondroitin sulfate proteoglycans which are produced by reactive glial cells, including astrocytes [19, 21]. In addition, these proteoglycans impede process outgrowth of oligodendrocytes and thereby disturb remyelination [50, 51]. Based on the dual character of astrocytes, it has been suggested that they can be classified into a neurotoxic A1 and neuroprotective A2 phenotype [24, 25]. Different factors, such as chemokines and cytokines, e.g., IL-1 β , TNF- α , and IL-10, have been found to control the development of astrocytes in the direction of either phenotype [25, 52, 53]. One of the regulators of astrocyte polarization is LCN2 which supports the pro-inflammatory A1 phenotype and decreases the polarization in the direction of A2 *in vitro* by inhibiting IL-4–STAT6 signaling [25]. The influence of LCN2 on astrocyte polarization, morphology, and migration is an important aspect of its regulatory function in neuroinflammation [27, 54]. LCN2 is involved in various pathological processes, such as stroke, metabolic inflammation, diabetes, and nonalcoholic steatohepatitis [30, 31, 55, 56]. It promotes inflammation through induction of pro-inflammatory cytokines via release of high mobility group box 1, which binds to toll-like receptor 4 and induces oxidative stress by activation of NOX-2 signaling [55]. Furthermore, beyond its effect on activation and polarization of microglia, LCN2 supports the recruitment of inflammatory cells by the induction of CXCL10 secretion and release of the neutrophil-recruitment signal IL-8 [31, 34, 57–59].

In the present study, we could demonstrate that SCI induces an increase of *Lcn2* expression throughout the whole SC. As the cellular source of LCN2 in the CNS, previous studies have identified astrocytes and endothelial cells [26, 60]. As already described in a stroke mouse model and in a SCI contusion mouse model similar to the animal model used in our study, we also recognized a co-localization of GFAP and LCN2 in some cells [26, 30].

After SCI, leukocytes are recruited to the lesion region within hours [61]. According to our results from co-staining against CD44 and LCN2, the major source of local LCN2 seems to be infiltrated leukocytes, as most LCN2-positive cells are also positive for the leukocyte marker CD44 [62]. However, we could not prove the production of LCN2 by microglia in our animal model [63]. The triggers of LCN2 production in this context are, besides others, cytokines such as IL-6 and NF-kappa B activation [60, 64].

Since LCN2 is secreted, and elevated concentrations can be found in the blood circulation under pathological conditions, like multiple sclerosis, intestinal inflammation, and arthritic diseases, it has been described as a biomarker in several pathologies [65]. In the present study, we show that the LCN2 concentration is significantly increased in the serum as a direct consequence of SCI, which might suggest this molecule as a potential biomarker for traumatic SCI. Furthermore, circulating LCN2 could be considered a part of the systemic inflammatory response (SIR) which affects the homeostasis of peripheral organs such as the liver, kidney, lung, and intestine. Thereby, it contributes to the pathogenesis of multiple organ dysfunction after SCI and supports secondary injury to the SC [38, 66–69]. In addition, we were able to detect elevated LCN2 levels in the brain and liver. This can have at least two reasons: As a first possibility, LCN2 might be produced in the respective tissue. This is supported by the fact that we have found significantly increased *Lcn2* mRNA in both brain and liver. Additionally, the identification of LCN2+ cells in both tissues after IHC staining indicates a production of LCN2 by the resident cells. In the brain, we could identify endothelial cells as a cellular source of LCN2 by double immunofluorescence staining. One of the possible triggers of LCN2 production in the brain is cytokines. For example, the *i.p.* application of IL-6 induces LCN2 production by vascular cells in the brain in mice [60]. In adipocytes also, TNF- α and IL-1 β trigger LCN2 production *in vitro* [70]. Since various cytokines have been shown to be upregulated in the blood stream after SCI, they might lead to an increase in LCN2 production in endothelial cells [71].

In the liver, hepatocytes and neutrophil granulocytes have been identified as cellular sources of LCN2 [72, 73]. It has been demonstrated *in vitro* that the cytokine IL-1 β induces LCN2 production in a NF-kappa B-dependent manner in both cell types [74–76]. Due to the structure of the hepatic

tissue, hepatocytes and recruited neutrophils come into close contact with cytokines, reaching the liver via the hepatic artery which might induce LCN2 production [77]. Since we have found elevated LCN2 levels in serum post SCI, LCN2 might also, besides its production by resident cells, reach the brain and the liver via the bloodstream.

In the brain, LCN2 has different beneficial as well as harmful effects [78]. In the ischemic brain, LCN2 contributes to neuronal cell death by promoting neuroinflammation [79]. However, in an experimental model of multiple sclerosis, *Lcn2*-deficient mice exhibited increased disease severity, suggesting a neuroprotective role of LCN2 [46]. In liver pathology, the effects of LCN2 have been discussed controversially. In phases of acute liver injury, LCN2 plays an essential role in liver homeostasis and lipid metabolism and protects hepatocytes, whereas it promotes liver injury and hepatic steatosis in a model of alcoholic steatohepatitis [80–82].

In our studies, the decrease of the astrogliosis marker Gfap in *Lcn2*^{-/-} mice is a first, valuable hint at a possible promotion of astrogliosis by LCN2 in SCI [83]. This assumption is further supported by the decrease in astrogliosis in the central spinal cord region in *Lcn2*^{-/-} compared to WT at 7 days demonstrated by immunohistochemical staining shown in Supplementary Fig. 2. In vitro, it has already been demonstrated that Gfap expression is promoted by LCN2 [84]. However, according to our results, LCN2 does not affect the regulatory mechanism underlying the phenotypic polarization of activated astrocytes in our animal model. The promotion of the classical inflammatory activation of astrocytes by LCN2 has, up to now, been only confirmed in vitro and in an animal model of transient middle cerebral artery occlusion [25, 85]. Eventually, the effect of LCN2 on astrocyte polarization depends on the underlying pathology.

So far, we base our conclusions regarding the influence of LCN2 on astrogliosis and astrocyte polarization on qPCR studies. Therefore, possible posttranslational modifications cannot be taken into account. This limitation has to be addressed in further studies. Nevertheless, we confirm a general positive effect of *Lcn2* deficiency on the functional outcome in SCI based on BBB locomotor scoring. It is assumed that the elevated level of LCN2 after SCI may exacerbate axonal degeneration and contribute to poor neurological outcome by enhancing inflammatory cell infiltration and promoting neuronal apoptosis [26].

In summary, we found that SCI promotes the LCN2-upregulation in SC, brain, blood circulation, and peripheral organs such as the liver. Consequently, LCN2 might play a role in systemic effects and multiple organ dysfunction in SCI pathology. The precise effect of LCN2 on peripheral organs has to be examined thoroughly to understand the resulting SCI-induced impairment of these

tissues. As a local consequence of SCI pathology, LCN2 promotes specific aspects of astrogliosis, which suggests that LCN2 can be therapeutically targeted to modulate the reaction of astrocytes in certain pathologies such as SCI. Further studies are needed to elucidate the precise mechanisms responsible for astrocyte activation and polarization to better understand the role played by LCN2 in this process.

Supplementary Information The online version contains supplementary material available at <https://doi.org/10.1007/s12035-021-02530-7>.

Acknowledgements We thank Uta Zahn, Petra Ibold, and Helga Helten for their technical support. Furthermore, we would like to acknowledge Tak W Mak, (University of Toronto, Canada) for providing *Lcn2* knockout animals.

Author Contribution The study was conceptualized and designed by Adib Zendedel, Cordian Beyer, Tim Clarner, and Victoria Behrens. Material preparation, data collection, and analysis were performed by Victoria Behrens, Weiyi Zhao, Clara Voelz, Nina Müller, and Natalie Gasterich. The first draft of the manuscript was written by Victoria Behrens, and all authors commented on previous versions of the manuscript. All authors read and approved the final manuscript. Adib Zendedel was responsible for the overall supervision of this study.

Funding This project was supported by an internal grant from RWTH Aachen University (A. Zendedel, START- 101/18).

Data Availability The datasets generated and analyzed during this study are available from the corresponding author upon reasonable request.

Code Availability Not applicable.

Declarations

Ethics Approval All animals used in this study were acquired and cared for in accordance with the Federation of European Laboratory Associations (FELASA) recommendations. All experimental procedures and animal care were approved by the Review board for the Care of Animal Subjects of the district government (LANUV, Recklinghausen, North Rhine-Westphalia, Germany) or by the Review Board for the Care of Animal Subjects of the district government (ethic No. 962055, Tehran, Iran) respectively.

Consent to Participate Not applicable.

Consent for Publication Not applicable.

Conflict of Interest The authors declare no competing interests.

References

- Westgren N, Levi R (1998) Quality of life and traumatic spinal cord injury. *Arch Phys Med Rehabil* 79(11):1433–1439. [https://doi.org/10.1016/s0003-9993\(98\)90240-4](https://doi.org/10.1016/s0003-9993(98)90240-4)

2. Torregrossa F, Salli M, Grasso G (2020) Emerging therapeutic strategies for traumatic spinal cord injury. *World Neurosurg* 140:591–601. <https://doi.org/10.1016/j.wneu.2020.03.199>
3. Ahuja CS et al (2017) Traumatic spinal cord injury-repair and regeneration. *Neurosurgery* 80(3S):S9–S22. <https://doi.org/10.1093/neuros/nyw080>
4. Fleming JC et al (2006) The cellular inflammatory response in human spinal cords after injury. *Brain* 129(Pt 12):3249–3269. <https://doi.org/10.1093/brain/awl296>
5. Gattlen C et al (2016) Spinal cord T-cell infiltration in the rat spared nerve injury model: a time course study. *Int J Mol Sci* 17(3):352. <https://doi.org/10.3390/ijms17030352>
6. Faulkner JR et al (2004) Reactive astrocytes protect tissue and preserve function after spinal cord injury. *J Neurosci* 24(9):2143–2155. <https://doi.org/10.1523/JNEUROSCI.3547-03.2004>
7. Sekhon LH, Fehlings MG (2001) Epidemiology, demographics, and pathophysiology of acute spinal cord injury. *Spine (Phila Pa 1976)* 26(24 Suppl):S2–12. <https://doi.org/10.1097/00007632-200112151-00002>
8. Ducker TB, Assenmacher DR (1969) Microvascular response to experimental spinal cord trauma. *Surg Forum* 20:428–430
9. Guha A, Tator CH (1988) Acute cardiovascular effects of experimental spinal cord injury. *J Trauma* 28(4):481–490. <https://doi.org/10.1097/00005373-198804000-00011>
10. Pineau I et al (2010) Astrocytes initiate inflammation in the injured mouse spinal cord by promoting the entry of neutrophils and inflammatory monocytes in an IL-1 receptor/MyD88-dependent fashion. *Brain Behav Immun* 24(4):540–553. <https://doi.org/10.1016/j.bbi.2009.11.007>
11. David S, Kroner A (2011) Repertoire of microglial and macrophage responses after spinal cord injury. *Nat Rev Neurosci* 12(7):388–399. <https://doi.org/10.1038/nrn3053>
12. Taoka Y et al (1997) Role of neutrophils in spinal cord injury in the rat. *Neuroscience* 79(4):1177–1182. [https://doi.org/10.1016/s0306-4522\(97\)00011-0](https://doi.org/10.1016/s0306-4522(97)00011-0)
13. Popovich PG et al (1999) Depletion of hematogenous macrophages promotes partial hindlimb recovery and neuroanatomical repair after experimental spinal cord injury. *Exp Neurol* 158(2):351–365. <https://doi.org/10.1006/exnr.1999.7118>
14. Cregg JM et al (2014) Functional regeneration beyond the glial scar. *Exp Neurol* 253:197–207. <https://doi.org/10.1016/j.expneurol.2013.12.024>
15. Kroner AJ (2019) Rosas Almanza, *Role of microglia in spinal cord injury*. *Neurosci Lett* 709:134370. <https://doi.org/10.1016/j.neulet.2019.134370>
16. Haydon PG, Carmignoto G (2006) Astrocyte control of synaptic transmission and neurovascular coupling. *Physiol Rev* 86(3):1009–1031. <https://doi.org/10.1152/physrev.00049.2005>
17. Bush TG et al (1999) Leukocyte infiltration, neuronal degeneration, and neurite outgrowth after ablation of scar-forming, reactive astrocytes in adult transgenic mice. *Neuron* 23(2):297–308. [https://doi.org/10.1016/s0896-6273\(00\)80781-3](https://doi.org/10.1016/s0896-6273(00)80781-3)
18. Firkins SS, Bates CA, Stelzner DJ (1993) Corticospinal tract plasticity and astroglial reactivity after cervical spinal injury in the postnatal rat. *Exp Neurol* 120(1):1–15. <https://doi.org/10.1006/exnr.1993.1036>
19. Davies SJ et al (1997) Regeneration of adult axons in white matter tracts of the central nervous system. *Nature* 390(6661):680–683. <https://doi.org/10.1038/37776>
20. Okada S et al (2006) Conditional ablation of Stat3 or Socs3 discloses a dual role for reactive astrocytes after spinal cord injury. *Nat Med* 12(7):829–834. <https://doi.org/10.1038/nm1425>
21. Bellver-Landete V et al (2019) Microglia are an essential component of the neuroprotective scar that forms after spinal cord injury. *Nat Commun* 10(1):518. <https://doi.org/10.1038/s41467-019-08446-0>
22. Zamanian JL et al (2012) Genomic analysis of reactive astrogliosis. *J Neurosci* 32(18):6391–6410. <https://doi.org/10.1523/JNEUROSCI.6221-11.2012>
23. Brambilla R et al (2005) Inhibition of astroglial nuclear factor kappaB reduces inflammation and improves functional recovery after spinal cord injury. *J Exp Med* 202(1):145–156. <https://doi.org/10.1084/jem.20041918>
24. Liddel SA et al (2017) Neurotoxic reactive astrocytes are induced by activated microglia. *Nature* 541(7638):481–487. <https://doi.org/10.1038/nature21029>
25. Jang E et al (2013) Phenotypic polarization of activated astrocytes: the critical role of lipocalin-2 in the classical inflammatory activation of astrocytes. *J Immunol* 191(10):5204–5219. <https://doi.org/10.4049/jimmunol.1301637>
26. Rathore KI et al (2011) Lipocalin 2 plays an immunomodulatory role and has detrimental effects after spinal cord injury. *J Neurosci* 31(38):13412–13419. <https://doi.org/10.1523/jneurosci.0116-11.2011>
27. Flo TH et al (2004) Lipocalin 2 mediates an innate immune response to bacterial infection by sequestering iron. *Nature* 432(7019):917–921. <https://doi.org/10.1038/nature03104>
28. Al Nimer F et al (2016) Lipocalin-2 is increased in progressive multiple sclerosis and inhibits remyelination. *Neuro Neuroimmunol Neuroinflamm* 3(1):e191. <https://doi.org/10.1212/NXI.000000000000191>
29. Ni W et al (2015) Role of lipocalin-2 in brain injury after intracerebral hemorrhage. *J Cereb Blood Flow Metab* 35(9):1454–1461. <https://doi.org/10.1038/jcbfm.2015.52>
30. Ranjbar Taklimie F et al (2019) Hypoxia induces astrocyte-derived lipocalin-2 in ischemic stroke. *Int J Mol Sci* 20(6). <https://doi.org/10.3390/ijms20061271>
31. Moschen AR et al (2017) Lipocalin-2: a master mediator of intestinal and metabolic inflammation. *Trends Endocrinol Metab* 28(5):388–397. <https://doi.org/10.1016/j.tem.2017.01.003>
32. Yang J et al (2002) An iron delivery pathway mediated by a lipocalin. *Mol Cell* 10(5):1045–1056. [https://doi.org/10.1016/s1097-2765\(02\)00710-4](https://doi.org/10.1016/s1097-2765(02)00710-4)
33. Bi F et al (2013) Reactive astrocytes secrete lcn2 to promote neuron death. *Proc Natl Acad Sci U S A* 110(10):4069–4074. <https://doi.org/10.1073/pnas.1218497110>
34. Jang E et al (2013) Secreted protein lipocalin-2 promotes microglial M1 polarization. *FASEB J* 27(3):1176–1190. <https://doi.org/10.1096/fj.12-222257>
35. Wu J et al (2014) Spinal cord injury causes brain inflammation associated with cognitive and affective changes: role of cell cycle pathways. *J Neurosci* 34(33):10989–11006. <https://doi.org/10.1523/JNEUROSCI.5110-13.2014>
36. Davidoff G et al (1985) Cognitive dysfunction and mild closed head injury in traumatic spinal cord injury. *Arch Phys Med Rehabil* 66(8):489–491
37. Davidoff GN, Roth EJ, Richards JS (1992) Cognitive deficits in spinal cord injury: epidemiology and outcome. *Arch Phys Med Rehabil* 73(3):275–284
38. Campbell SJ et al (2005) Central nervous system injury triggers hepatic CC and CXC chemokine expression that is associated with leukocyte mobilization and recruitment to both the central nervous system and the liver. *Am J Pathol* 166(5):1487–1497. [https://doi.org/10.1016/s0002-9440\(10\)62365-6](https://doi.org/10.1016/s0002-9440(10)62365-6)
39. Cheng RD et al (2020) Spinal cord injury causes insulin resistance associated with PI3K signaling pathway in hypothalamus. *Neurochem Int* 140:104839. <https://doi.org/10.1016/j.neuint.2020.104839>

40. Berger T et al (2006) Lipocalin 2-deficient mice exhibit increased sensitivity to *Escherichia coli* infection but not to ischemia-reperfusion injury. *Proc Natl Acad Sci U S A* 103(6):1834–1839. <https://doi.org/10.1073/pnas.0510847103>
41. Gasterich N et al (2021) Inflammatory responses of astrocytes are independent from lipocalin 2. *J Mol Neurosci* 71(5):933–942. <https://doi.org/10.1007/s12031-020-01712-7>
42. Basso DM, Beattie MS, Bresnahan JC (1995) A sensitive and reliable locomotor rating scale for open field testing in rats. *J Neurotrauma* 12(1):1–21. <https://doi.org/10.1089/neu.1995.12.1>
43. Livak KJ, Schmittgen TD (2001) Analysis of relative gene expression data using real-time quantitative PCR and the 2(-Delta Delta C(T)) Method. *Methods* 25(4):402–408. <https://doi.org/10.1006/meth.2001.1262>
44. Neal M et al (2018) Prokineticin-2 promotes chemotaxis and alternative A2 reactivity of astrocytes. *Glia* 66(10):2137–2157. <https://doi.org/10.1002/glia.23467>
45. Dekens DW et al (2017) Neutrophil gelatinase-associated lipocalin and its receptors in Alzheimer's disease (AD) brain regions: differential findings in AD with and without depression. *J Alzheimers Dis* 55(2):763–776. <https://doi.org/10.3233/JAD-160330>
46. Berard JL et al (2012) Lipocalin 2 is a novel immune mediator of experimental autoimmune encephalomyelitis pathogenesis and is modulated in multiple sclerosis. *Glia* 60(7):1145–1159. <https://doi.org/10.1002/glia.22342>
47. O'Shea TM, Burda JE, Sofroniew MV (2017) Cell biology of spinal cord injury and repair. *J Clin Invest* 127(9):3259–3270. <https://doi.org/10.1172/JCI90608>
48. Freeman KA et al (2015) Spinal cord protection via alpha-2 agonist-mediated increase in glial cell-line-derived neurotrophic factor. *J Thorac Cardiovasc Surg* 149(2):578–84 discussion 584–6. <https://doi.org/10.1016/j.jtcvs.2014.10.037>
49. Sofroniew MV (2014) Multiple roles for astrocytes as effectors of cytokines and inflammatory mediators. *Neuroscientist* 20(2):160–172. <https://doi.org/10.1177/1073858413504466>
50. Siebert JR, Osterhout DJ (2011) The inhibitory effects of chondroitin sulfate proteoglycans on oligodendrocytes. *J Neurochem* 119(1):176–188. <https://doi.org/10.1111/j.1471-4159.2011.07370.x>
51. Tran AP, Warren PM, Silver J (2018) The biology of regeneration failure and success after spinal cord injury. *Physiol Rev* 98(2):881–917. <https://doi.org/10.1152/physrev.00017.2017>
52. Liu LR et al (2020) Interaction of microglia and astrocytes in the neurovascular unit. *Front Immunol* 11:1024. <https://doi.org/10.3389/fimmu.2020.01024>
53. Hyvarinen T et al (2019) Co-stimulation with IL-1beta and TNF-alpha induces an inflammatory reactive astrocyte phenotype with neurosupportive characteristics in a human pluripotent stem cell model system. *Sci Rep* 9(1):16944. <https://doi.org/10.1038/s41598-019-53414-9>
54. Lee S, Jha MK, Suk K (2015) Lipocalin-2 in the inflammatory activation of brain astrocytes. *Crit Rev Immunol* 35(1):77–84. <https://doi.org/10.1615/critrevimmunol.2015012127>
55. Mondal A et al (2020) Lipocalin 2 induces neuroinflammation and blood-brain barrier dysfunction through liver-brain axis in murine model of nonalcoholic steatohepatitis. *J Neuroinflammation* 17(1):201. <https://doi.org/10.1186/s12974-020-01876-4>
56. Rashad NM et al (2017) Lipocalin-2 expression and serum levels as early predictors of type 2 diabetes mellitus in obese women. *IUBMB Life* 69(2):88–97. <https://doi.org/10.1002/iub.1594>
57. Shashidharamurthy R et al (2013) Differential role of lipocalin 2 during immune complex-mediated acute and chronic inflammation in mice. *Arthritis Rheum* 65(4):1064–1073. <https://doi.org/10.1002/art.37840>
58. Lee S et al (2011) Lipocalin-2 Is a chemokine inducer in the central nervous system: role of chemokine ligand 10 (CXCL10) in lipocalin-2-induced cell migration. *J Biol Chem* 286(51):43855–43870. <https://doi.org/10.1074/jbc.M111.299248>
59. Bachman MA, Miller VL, Weiser JN (2009) Mucosal lipocalin 2 has pro-inflammatory and iron-sequestering effects in response to bacterial enterobactin. *PLoS Pathog* 5(10):e1000622. <https://doi.org/10.1371/journal.ppat.1000622>
60. Hamzic N, Blomqvist A, Nilsberth C (2013) Immune-induced expression of lipocalin-2 in brain endothelial cells: relationship with interleukin-6, cyclooxygenase-2 and the febrile response. *J Neuroendocrinol* 25(3):271–280. <https://doi.org/10.1111/jne.12000>
61. Noble LJ et al (2002) Matrix metalloproteinases limit functional recovery after spinal cord injury by modulation of early vascular events. *J Neurosci* 22(17):7526–7535
62. Johnson P et al (2000) A role for the cell adhesion molecule CD44 and sulfation in leukocyte-endothelial cell adhesion during an inflammatory response? *Biochem Pharmacol* 59(5):455–465. [https://doi.org/10.1016/s0006-2952\(99\)00266-x](https://doi.org/10.1016/s0006-2952(99)00266-x)
63. Lee S et al (2007) A dual role of lipocalin 2 in the apoptosis and deramification of activated microglia. *J Immunol* 179(5):3231–3241. <https://doi.org/10.4049/jimmunol.179.5.3231>
64. Ouali Alami N et al (2018) NF-kappaB activation in astrocytes drives a stage-specific beneficial neuroimmunological response in ALS. *EMBO J* 37(16). <https://doi.org/10.15252/embj.201798697>
65. Abella V et al (2015) The potential of lipocalin-2/NGAL as biomarker for inflammatory and metabolic diseases. *Biomarkers* 20(8):565–571. <https://doi.org/10.3109/1354750X.2015.1123354>
66. Gris D, Hamilton EF, Weaver LC (2008) The systemic inflammatory response after spinal cord injury damages lungs and kidneys. *Exp Neurol* 211(1):259–270. <https://doi.org/10.1016/j.expneurol.2008.01.033>
67. Zhang C et al (2018) Gut microbiota dysbiosis in male patients with chronic traumatic complete spinal cord injury. *J Transl Med* 16(1):353. <https://doi.org/10.1186/s12967-018-1735-9>
68. Campbell IL (2005) Cytokine-mediated inflammation, tumorigenesis, and disease-associated JAK/STAT/SOCS signaling circuits in the CNS. *Brain Res Brain Res Rev* 48(2):166–177. <https://doi.org/10.1016/j.brainresrev.2004.12.006>
69. Sundman MH et al (2017) The bidirectional gut-brain-microbiota axis as a potential nexus between traumatic brain injury, inflammation, and disease. *Brain Behav Immun* 66:31–44. <https://doi.org/10.1016/j.bbi.2017.05.009>
70. Zhang Y et al (2014) Lipocalin 2 expression and secretion is highly regulated by metabolic stress, cytokines, and nutrients in adipocytes. *PLoS One* 9(5):e96997. <https://doi.org/10.1371/journal.pone.0096997>
71. Mukhamedshina YO et al (2017) Systemic and local cytokine profile following spinal cord injury in rats: a multiplex analysis. *Front Neurol* 8:581. <https://doi.org/10.3389/fneur.2017.00581>
72. Molina L et al (2018) Hepatocyte-derived lipocalin 2 is a potential serum biomarker reflecting tumor burden in hepatoblastoma. *Am J Pathol* 188(8):1895–1909. <https://doi.org/10.1016/j.ajpath.2018.05.006>
73. Li H et al (2018) Hepatocytes and neutrophils cooperatively suppress bacterial infection by differentially regulating lipocalin-2 and neutrophil extracellular traps. *Hepatology* 68(4):1604–1620. <https://doi.org/10.1002/hep.29919>
74. Jayaraman A et al (2005) Identification of neutrophil gelatinase-associated lipocalin (NGAL) as a discriminatory marker of the hepatocyte-secreted protein response to IL-1beta: a proteomic analysis. *Biotechnol Bioeng* 91(4):502–515. <https://doi.org/10.1002/bit.20535>
75. Cowland JB et al (2003) Neutrophil gelatinase-associated lipocalin is up-regulated in human epithelial cells by IL-1 beta, but not by

- TNF- α . *J Immunol* 171(12):6630–6639. <https://doi.org/10.4049/jimmunol.171.12.6630>
76. Borkham-Kamphorst E, Drews F, Weiskirchen R (2011) Induction of lipocalin-2 expression in acute and chronic experimental liver injury moderated by pro-inflammatory cytokines interleukin-1 β through nuclear factor- κ B activation. *Liver Int* 31(5):656–665. <https://doi.org/10.1111/j.1478-3231.2011.02495.x>
77. Fleming JC et al (2012) Remote inflammatory response in liver is dependent on the segmental level of spinal cord injury. *J Trauma Acute Care Surg* 72(5):1194–201 discussion 1202. <https://doi.org/10.1097/TA.0b013e31824d68bd>
78. Ferreira AC et al (2015) From the periphery to the brain: Lipocalin-2, a friend or foe? *Prog Neurobiol* 131:120–136. <https://doi.org/10.1016/j.pneurobio.2015.06.005>
79. Jin M et al (2014) Lipocalin-2 deficiency attenuates neuroinflammation and brain injury after transient middle cerebral artery occlusion in mice. *J Cereb Blood Flow Metab* 34(8):1306–1314. <https://doi.org/10.1038/jcbfm.2014.83>
80. Borkham-Kamphorst E et al (2013) Protective effects of lipocalin-2 (LCN2) in acute liver injury suggest a novel function in liver homeostasis. *Biochim Biophys Acta* 1832(5):660–673. <https://doi.org/10.1016/j.bbadis.2013.01.014>
81. Asimakopoulou A et al (2014) Lipocalin-2 (LCN2) regulates PLIN5 expression and intracellular lipid droplet formation in the liver. *Biochim Biophys Acta* 1842(10):1513–1524. <https://doi.org/10.1016/j.bbalip.2014.07.017>
82. Wieser V et al (2016) Lipocalin 2 drives neutrophilic inflammation in alcoholic liver disease. *J Hepatol* 64(4):872–880. <https://doi.org/10.1016/j.jhep.2015.11.037>
83. Li T et al (2019) An update on reactive astrocytes in chronic pain. *J Neuroinflammation* 16(1):140. <https://doi.org/10.1186/s12974-019-1524-2>
84. Lee S et al (2009) Lipocalin-2 is an autocrine mediator of reactive astrogliosis. *J Neurosci* 29(1):234–249. <https://doi.org/10.1523/JNEUROSCI.5273-08.2009>
85. Zhao N et al (2019) Lipocalin-2 may produce damaging effect after cerebral ischemia by inducing astrocytes classical activation. *J Neuroinflammation* 16(1):168. <https://doi.org/10.1186/s12974-019-1556-7>
86. Franklin KBJ, Paxinos G (2019) Paxinos and Franklin's the mouse brain in stereotaxic coordinates. Academic Press, Cambridge, United States

Publisher's Note Springer Nature remains neutral with regard to jurisdictional claims in published maps and institutional affiliations.